

Photoproduction with a mini-jet model and Cosmic Ray showers

*F. Cornet*¹, *C. Garcia-Canal*², *A. Grau*¹, *G. Pancheri*^{3*}, *S. J. Sciutto*²

¹ Departamento de Física Teórica y del Cosmos, Universidad de Granada, E-18071 Granada, Spain

² Departamento de Física, Universidad Nacional de La Plata, IFLP, CONICET, C. C. 67, 1900 La Plata, Argentina

³ INFN Frascati, National Laboratories, Frascati 00044, Italy

Abstract

We present post-LHC updates of estimates of the total photo-production cross section in a mini-jet model with infrared soft gluon resummation, and apply the model to study Cosmic Ray shower development, comparing the results with those obtained from other existing models.

Keywords

Total photo-production cross section; mini-jet models; cosmic rays; shower development

1 The total photo production cross section

We address again the question of how different models for photo production affect the description of the development of photon-initiated cosmic ray showers and, consequently, how much the estimated photon composition of the showers depends from the models used in the simulation. In this way, we update a previous publication [1]. The simulation of the shower development is performed using the AIRES MC [2], linked to the hadronic models QGSJET-II-04 [3], QGSJET in the following, and EPOS-LHC 3.40 [4], EPOS in the following, that have recently been updated to take into account LHC results. The study includes two different photo-production models:

- the Block and Halzen (BH) model for total cross sections at very high energies [5] presently in AIRES as default model,
- the extension to photoproduction [6] of the so-called Bloch-Nordsieck (BN) model for total hadronic cross sections [7, 8], recently implemented in AIRES.

1.1 The Bloch-Nordsieck (BN) model for hadronic processes

This model for the total hadronic cross section is based on a perturbative QCD (pQCD) calculation of mini-jets as being at the origin of the observed rise [9] of the total cross section with energy. For a fixed minimum transverse momentum of the scattering partons, called $p_{tmin} \gtrsim 1$ GeV, the low-x behavior of the PDFs leads to a very strong increase of the minijet integrated cross sections as the c.m. energy increases, shown in the left panel of Figure 1 for different LO Parton Density Functions (PDFs): Glück, Reya and Schienbein (GRS) [10] for the photon, Glück, Reya and Vogt (GRV) [11], and Martin, Roberts, Stirling and Thorne (MRST) [12] for the proton. In the BN model, to be described shortly, infrared gluon resummation tames the fast rise of mini-jet cross sections through soft gluon emissions and can lead to saturation through a phenomenological ansatz for resummation of $k_t \simeq 0$ gluons, which we outline below. Thus the sudden rise around $\sqrt{s} \gtrsim 10 - 20$ GeV morphs into the experimentally observed gentle asymptotic behaviour, which satisfies the Froissart-Martin bound, i.e. $\sigma_{total} \lesssim [\log s]^2$. To this effect,

*Research affiliate with MIT CTP, Cambridge, MA, USA

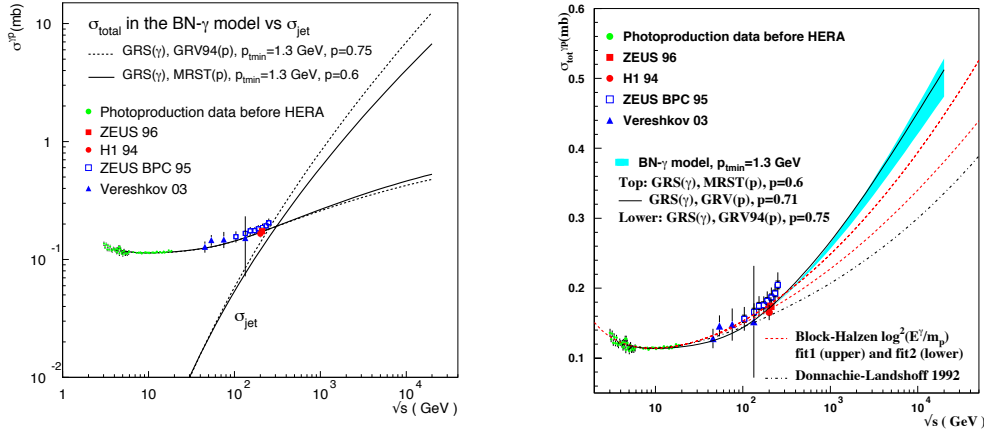


Fig. 1: Left panel: Mini-jet integrated cross sections for different PDFs in γp scattering, in comparison with γp total cross section data and the BN model described in the text. Right panel: Total γp cross section calculated for different PDFs with the BN model, called here BN- γ , and compared with the model of Ref. [5], with lower red dashed curve being the default in AIRES, and the Donnachie and Landshoff description of Ref. [13].

mini-jet collisions are embedded into the eikonal formulation for the total cross section, which, for pp scattering, reads as

$$\sigma_{total} = 2 \int d^2\mathbf{b} [1 - e^{-[\bar{n}_{soft}(b,s) + \bar{n}_{hard}(b,s)]/2}] \quad (1)$$

Here $\bar{n}_{hard}(b, s)$ is to be calculated through the LO, DGLAP evolved QCD jet cross section, while our choice for \bar{n}_{soft} is to parametrize it by normalizing σ_{total} at low energy, i.e. before pQCD mini-jet production takes up a major role. Phenomenology suggests that this quantity is either a constant or decreases with energy. On the other hand, the main point of the model used here is that $\bar{n}_{hard}(b, s)$ should be fully estimated by means of a pQCD calculation, with saturation effects due to an All Order Resummation procedure, which includes the infrared region.

Once pQCD can be applied, a complete description requires not only the calculation of hard parton-parton scattering but also soft gluon effects accompanying the collision. If, in Eq. (1), we write

$$\bar{n}_{hard}(b, s) = A_{hard}(b, s) \sigma_{jet}(s; p_{tmin}, PDFs) \quad (2)$$

then $A_{hard}(b, s)$ will include soft gluon resummation effects, and thus account for the cut-off in impact parameter space, required for satisfaction of the Froissart bound, i.e. the saturation effects.

Our model for resummation of soft gluons is based on a semi-classical approach in which one does not count individual gluons, hence no branching or angular ordering is involved, and follows the Bloch and Nordsieck observation [14] that soft photons emission follows a Poisson distribution and only an infinite number of them can give a finite cross section. The procedure to apply this result to QCD was first discussed in [15] and recently outlined in Ref [16]. Labelling as A_{BN} the impact parameter distribution of partons to use in Eq. (2), the resulting expression is the following:

$$A_{BN}(b, s; p, p_{tmin}) = \frac{e^{-h(b,s;p,p_{tmin})}}{\int d^2\mathbf{b} e^{-h(b,s;p,p_{tmin})}} \equiv \quad (3)$$

$$\mathcal{N}(s, p_{tmin}) \int d^2\mathbf{K}_t e^{-i\mathbf{K}_t \cdot \mathbf{b}} \frac{d^2 P_{soft-resum}(\mathbf{K}_t, s; p_{tmin})}{d^2\mathbf{K}_t} \quad (4)$$

$$\quad (5)$$

with

$$h(b, s; p, p_{tmin}) = \frac{8}{3\pi^2} \int_0^{q_{max}} d^2\mathbf{k}_t [1 - e^{i\mathbf{k}_t \cdot \mathbf{b}}] \alpha_s(k_t^2) \frac{\ln(2q_{max}/k_t)}{k_t^2} \quad (6)$$

$$q_{max}(s; p_{tmin}, PDF) = \frac{\sqrt{s} \sum_{i,j} \int \frac{dx_1}{x_1} f_{i/a}(x_1) \int \frac{dx_2}{x_2} f_{j/b}(x_2) \sqrt{x_1 x_2} \int_{z_{min}}^1 dz (1-z)}{2 \sum_{i,j} \int \frac{dx_1}{x_1} f_{i/a}(x_1) \int \frac{dx_2}{x_2} f_{j/b}(x_2) \int_{z_{min}}^1 (dz)} \quad (7)$$

where the integration in Eq. (6) makes use of an ansatz of maximal singularity for the behavior of the coupling of infrared gluons to the source current, namely $\alpha_s(k_t \rightarrow 0) \propto (k_t^2/\Lambda^2)^{-p}$ with $p < 1/2 < 1$ [15], and q_{max} is calculated from the kinematics of single gluon emission [17].

In Reference [6] the model described above was applied to photon processes, using photon PDFs, and a suitable parametrization for the probability P_{had} that a photon behaves like a hadron, following the simple, but effective model proposed in Ref. [18]. In [6] the total photo production cross section was then calculated as follows:

$$\sigma_{total}^{\gamma p} = 2P_{had} \int d^2\mathbf{b} [1 - e^{-[2/3 \bar{n}_{soft}^{pp}(b,s) + \bar{n}_{hard}^{\gamma p}(b,s)]/2}] \quad (8)$$

with

$$\bar{n}_{hard}^{\gamma p}(b, s) = \frac{A_{BN}^{\gamma p}(b, s; p, p_{tmin}, PDF) \sigma_{jet}^{\gamma p}(s; p_{tmin}, PDF)}{P_{had}}. \quad (9)$$

The probability P_{had} can be extracted from Vector Meson Dominance models, and adjusting it to the normalization of data at low energy, we propose $P_{had} = 1/240$.

After determining the best set of parameters $\{p, p_{tmin}\}$ compatible with existing γp data, we show in the right hand panel of Figure 1 our present calculation [1] for the photo production total cross section, updated from [6] with more recent sets of proton PDFs, and compare it with the results of the models from Refs. [5] and [13].

2 Shower development with post LHC AIRES simulations

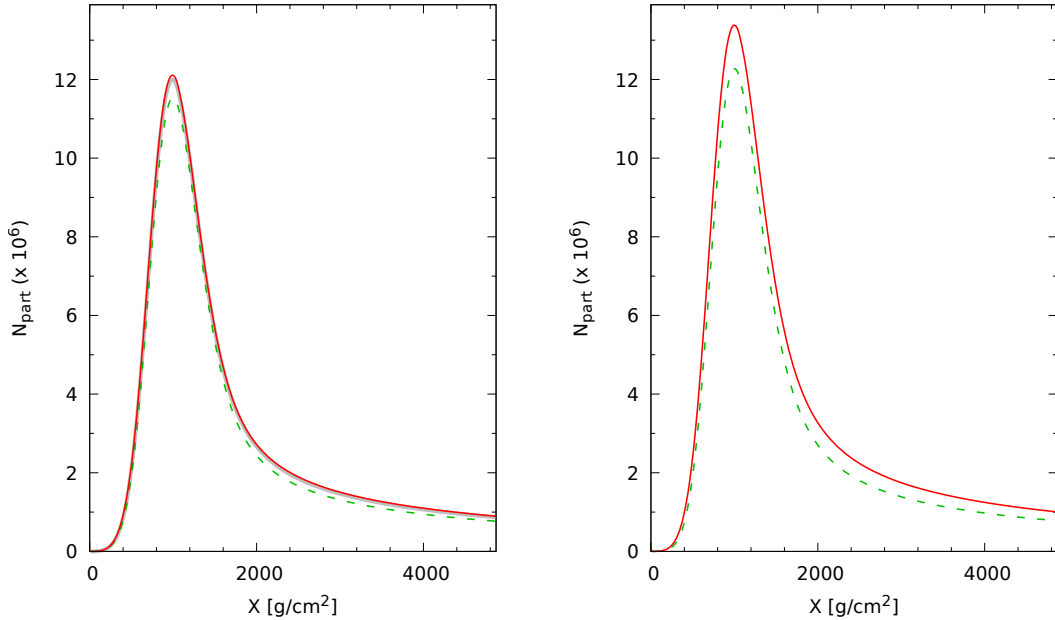


Fig. 2: Longitudinal development of muons for 10^{19} eV photon showers inclined 80 degrees. The solid (dashed) lines correspond to simulations with the BN- γ (BH) model for photonuclear cross section, and processing high energy hadronic interactions with the QGSJET-II-04 (left) and EPOS (right) models.

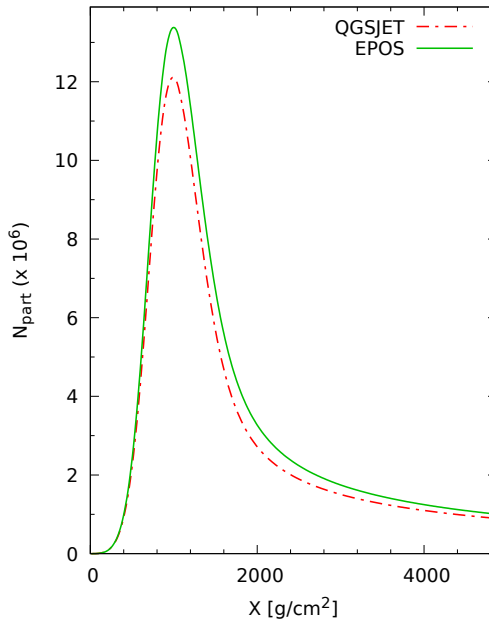


Fig. 3: Longitudinal development of muons for 10^{19} eV photon showers inclined 80 degrees from QGSJET-II-04 or EPOS 3.40 hadronic packages in the case of the BN- γ model for γp .

We have performed simulations of extended air showers using the AIRES system [2] linked to the packages QGSJET-II-04 [3] and EPOS 3.40 [4] for processing high energy hadronic interactions. The versions used for both hadronic models are those optimized taking into account the recent results of LHC experiments (for details see, for example, references [4, 19]).

With each of the mentioned hadronic models we have run two sets of simulations, namely, (1) using the cross sections for photonuclear reactions at energies greater than 200 GeV that are provided with the currently public version of AIRES which correspond to the lower of the two BH fits in the right panel of Figure 1 (model BH introduced in Section 1); and (2) replacing those cross sections by the ones corresponding to the present model [6] (model BN- γ introduced in Subsection 1.1).

Following the lines of our previous work [1], we report here on the results for the very representative case of 10^{19} eV gamma-initiated showers. As already pointed out in [1], at this primary energy, geomagnetic conversion [20] is not frequent, thus allowing photons to initiate normally the atmospheric shower development.

In Figures 2 and 3 the results for the longitudinal development of the mean number of muons is displayed, while in Figure 4 we present the results for the cases of pions and kaons.

For all the secondary particles considered, and for both hadronic models QGSJET and EPOS, the production of muons and hadrons is larger in the case of the simulations using the BN- γ model for photon cross sections, in comparison with the corresponding BH model results, as expected (see discussion in reference [1]). This shows up clearly in Figure 2 where the plots corresponding to the present model (solid red lines) are located always over those corresponding to the BH model (dashed green lines).

It is very important to notice that the number of hadrons produced during the shower development depends noticeably on the package used to process the hadronic collisions. Despite the fact that both hadronic packages have been tuned to best reproduce measurements performed at the LHC collider [4, 19], it is evident from the plots presented here that differences between models still persist. For example, the longitudinal profiles obtained using EPOS contain larger number of hadrons when compared with the

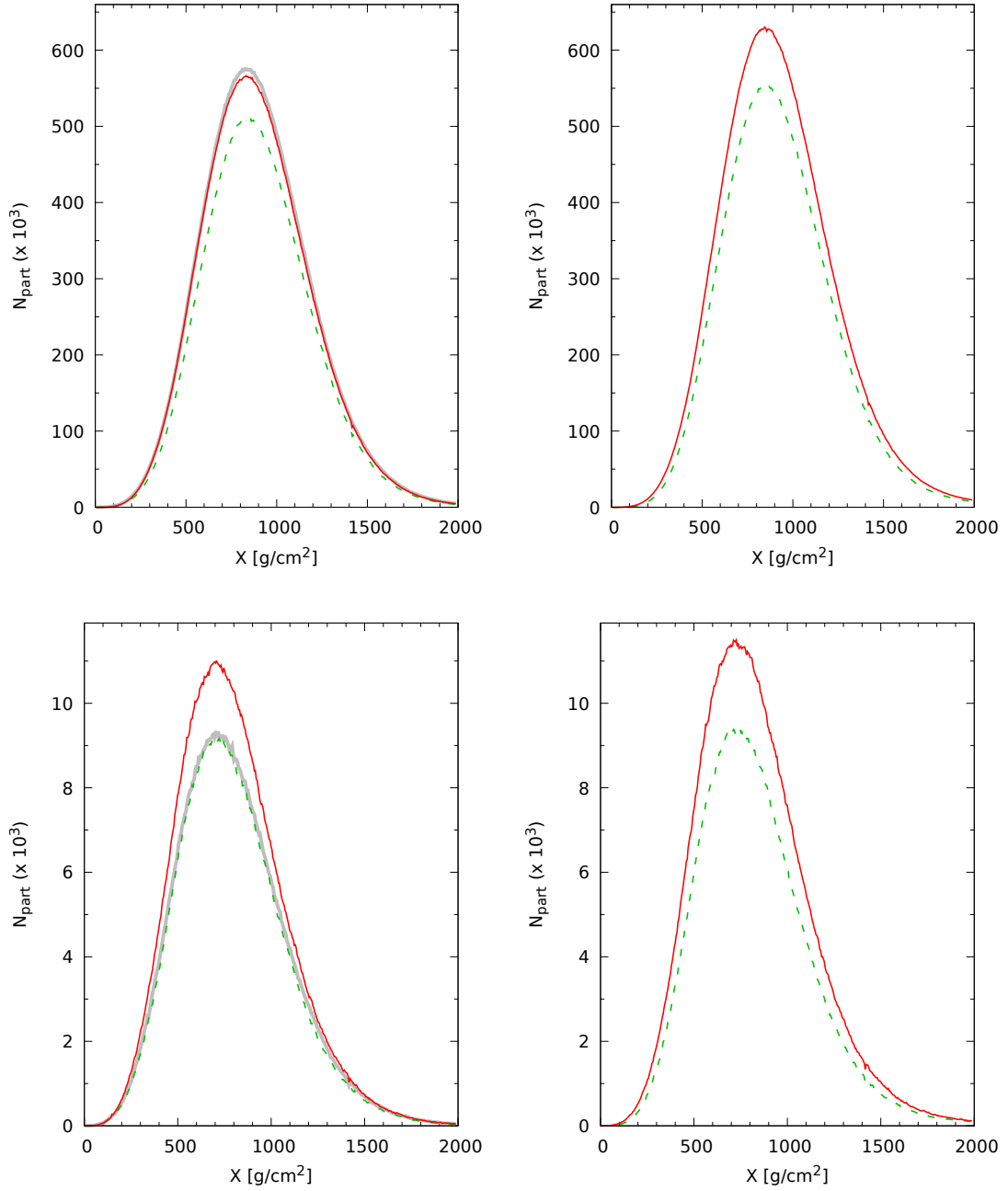


Fig. 4: Longitudinal development of pions (upper row) and kaons (lower row) for 10^{19} eV photon showers inclined 80 degrees. The solid (dashed) lines correspond to simulations with the present BN- γ (BH) model for photonuclear cross section, and processing high energy hadronic interactions with the QGSJET-II-04 (left) and EPOS (right) models. The grey line corresponds to similar simulations performed using the BN- γ model for photonuclear cross section and the (pre-LHC) QGSJET-II-03 model (see figure 6 of reference [1])

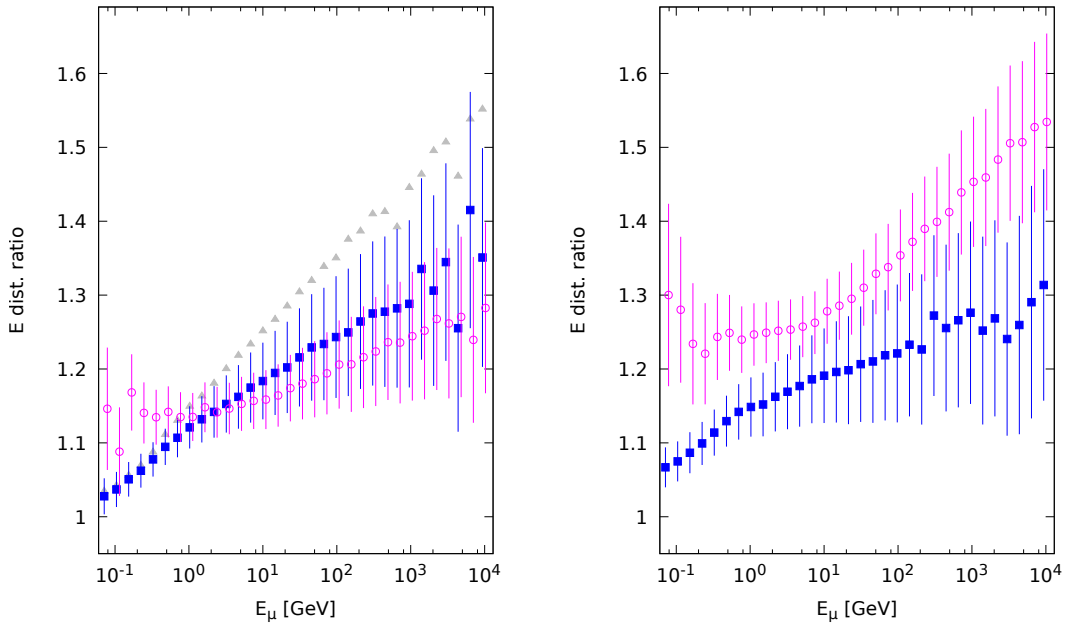


Fig. 5: Ratio between ground muon energy distributions obtained with the present (BN- γ) and old (BH) models, for 10^{19} eV photon showers, and simulating the hadronic simulations with QGSJET-II-04 (left) and EPOS (right). The solid squares (open circles) correspond to a shower inclination of 45 (80) deg. Error bars are calculated by propagation of the individual RMS statistical errors of each of the distributions. The abscissas of the 80 deg data set have been shifted by 10% to improve error bar visibility. The grey triangles correspond to similar simulations performed using the present BN- γ model for photonuclear cross section and the (pre-LHC) QGSJET-II-03 model for showers inclined 45 degrees (see figure 10 of reference [1]).

corresponding ones for the case of QGSJET. Using model BN- γ for photon cross sections (red solid lines in Figure 4), the number of pions at the point of maximum development is 11% larger for EPOS with respect to QGSJET. In the case of kaons such figure is only 1%, and for protons (neutrons) (not plotted) at the point of maximum development is 11% (8%) larger for EPOS-LHC with respect to QGSJET. As shower muons are generated after the decay of unstable hadrons, a similar increase can be seen for the maximum number of muons (Figure 2) where EPOS overpasses the prediction of QGSJET-II in 6%, as exemplified in Figure 3 for the case of muons when using model BN- γ for photon cross section.

Another point that is important to check is the difference between pre and post-LHC versions of each model. In Figure 4 we have included (grey lines in left column plots) the results corresponding to the present model for photon cross sections, but simulated using QGSJET-II-03 (pre-LHC version of QGSJET). These grey lines correspond to the respective solid red lines plotted in figures 5 and 6 of reference [1]. It can be observed that there are virtually no differences between the pre and post-LHC models in all the cases, except, remarkably, in the case of kaons (Figure 4 lower left plot), where the post-LHC model QGSJET-II-04 predicts a noticeably larger number of kaons.

Another quantity that we have included in our study is the ratio of energy distributions of muons reaching ground level (see the discussion on this quantity at reference [1]). Such ratios are plotted in Figure 5 as functions of the muon energy for the representative cases of 45 (solid squares) and 80 (open circles) degrees of inclination. The increased number of high energy muons resulting after the simulations using the BN- γ model for photonuclear cross sections shows up clearly. In the case of QGSJET (left) the increase of the number of muons is not much dependent on the inclination of the shower, and is noticeably smaller compared with the results corresponding to QGSJET-II-03 (grey triangles), already

studied in reference [1]. In the case of EPOS-LHC (right) the results are somewhat different with respect to the QGSJET ones. In this case the very inclined showers (80 degrees) present the largest increase rate, reaching nearly 50% for the most energetic muons, while for the showers inclined 45 degrees, the distribution ratios are about 25% for the most energetic muons.

The differences between the results obtained in our analysis using different hadronic models, indicate that the simulation of hadronic collisions at the highest energies continue to be an open issue, more than 30 years after the first simulations were reported, and despite all the experimental data that have been collected since then.

Acknowledgements

G.P. gratefully acknowledges hospitality at the MIT Center for Theoretical Physics. This work was partially supported by CONICET and ANPCyT, Argentina. A.G. acknowledges partial support by the Ministerio de Economía y Competitividad (Spain) under grant number FPA2016-78220-C3-3-P, and by Consejería de Economía, Innovación, Ciencia y Empleo, Junta de Andalucía (Spain)(Grants FQM 101 and FQM 6552). F. C. also acknowledges support by the Ministerio de Economía y Competitividad (Spain) under grant number FPA 2016-78220-C3-1-P, and by Consejería de Economía, Innovación, Ciencia y Empleo, Junta de Andalucía (Spain)(Grants FQM 330 and FQM 6552).

References

- [1] F. Cornet, C. A. Garcia Canal, A. Grau, G. Pancheri and S.J. Sciutto, *Phys. Rev.* **D92** (2015) 114011.
- [2] S. J. Sciutto, Proceedings of the 27th International Cosmic Ray Conference, Hamburg, 2001, p. 237; see also <http://www2.fisica.unlp.edu.ar/aires>.
- [3] S. Ostapchenko, *Phys. Rev.* **D83**, (2011) 014018; *Phys. Rev.* **D81**, (2010) 114028.
- [4] T. Pierog, I. Karpenko, J.M. Katzy, E. Yatsenko and K. Werner, *Phys. Rev.* **C92** (2015) 034906.
- [5] M.M. Block and F. Halzen *Phys. Rev.* **D70** (2004) 091901.
- [6] R.M. Godbole, A. Grau, G. Pancheri and Y.N. Srivastava, *Eur. Phys. J. C* **63** (2009) 69-85.
- [7] R.M. Godbole, A. Grau, G. Pancheri and Y.N. Srivastava, *Phys. Rev. D* **72** (2005) 076001.
- [8] A. Grau, G. Pancheri and Y.N. Srivastava, *Phys. Rev.* **D60** (1999) 114020.
- [9] Loyal Durand and Hong Pi, *Phys. Rev.* **D40** (1989) 1436.
- [10] M. Glück, E. Reya and I. Schienbein, *Phys. Rev.* **D60** (1999) 054019; Erratum:*Phys. Rev.* **D62** (2000) 019902.
- [11] M. Glück, E. Reya, and A. Vogt, *Z. Phys.* **C53** (1992) 127–134; *Z. Phys.* **C67** (1995) 443–448; *Eur. Phys. J.* **C5** (1998) 461–470.
- [12] A. D. Martin, R. G. Roberts, W. J. Stirling, and R. S. Thorne, *Phys. Lett.* **B531** (2002) 216–224.
- [13] A. Donnachie and P. V. Landshoff, *Phys.Lett.* **B296** (1992) 227-232.
- [14] F. Bloch, A. Nordsieck *Phys. Rev.* **52** (1937) 54-59.
- [15] A. Corsetti, A. Grau, G. Pancheri and Y.N. Srivastava, *Phys. Lett.* **B382** (1996) 282-288.
- [16] D. A. Fagundes, A. Grau, G. Pancheri, O. Shekhovtsova and Y. N. Srivastava, *Phys. Rev.* **D96** (2017) 054010.
- [17] P. Chiappetta and M. Greco, *Nucl. Phys.* **B199** (1982) 77.
- [18] R.S. Fletcher, T.K. Gaisser and F. Halzen, *Phys. Lett.* **B298** (1993) 442-444.
- [19] S. Ostapchenko, Proc. of the XXV European Cosmic Ray Symposium, Turin (2016), eConf C16-09-04.3, arXiv:1612.09461v1 [astro-ph.HE].
- [20] P. Billoir *et al.*, for The Pierre Auger Collaboration, Proceedings of the 27th International Cosmic Ray Conference, Hamburg, 2001, p. 718.